Calculation of Scattering Intensities for the Interaction of Light with a Cluster of Dielectric Objects

Emilie Huffman*
Union University

(Dated: August 12, 2011)

Abstract

The structure of the feather barbs of the avian species *Cotinga Cotinga* was modeled as a cluster of dielectric objects, and scattering theory was used to calculate scattering intensities of light incident on the structure from various angles. The strongest scattering intensities, regardless of the incident angle, were found in the 400-600 nm range, a finding consistent with experimental results. Evidence for iridescence from directional lighting was also found, a finding consistent with experiments involving quasi-ordered structures. The calculations revealed high intensities in a distinct range of the visible spectrum, suggesting that the quasi-ordered structures of the barbs have an ordered enough structure to produce wavelength specific color, however, the calculations also displayed a phi-dependence which must be removed in order to obtain truly accurate results.

1 Introduction

There has recently been a renewed interest across disciplines in the study of natural structural colors, which arise from the interaction of light with nanostructures. Developments such as photonic crystals, which are made up of periodic nanostructures have contributed to such interest.[2] Structural colors found in nature can be divided into classes: iridescent and non-iridescent. Iridescent colors will change with different viewing angles and are formed from an ordered, periodic array of scatterers. However, while non-iridescent colors–such as those found in the feathers of many birds–can arise from pigments, they also have been found to arise from quasi-ordered nanostructures in the barbs.[1] This paper calculates scattering intensities for light interacting with a quasi-ordered array of dielectric objects, specifically an array which models a feather barb of the avian species *Cotinga Cotinga*.

1.1 Quasi-Ordered Structures

The colors found in bird feathers are generated from the scattering of light off of the structures of the barbs, which consist of air vacuoles in the medullary keratin. In feathers lacking iridescence, it was thought that the air vacuoles always had to be randomly distributed so that the scattering of light depended solely on the properties of individual vacuoles, rather than from interference caused by order in the structure. However, Raman in 1935 challenged this idea by showing that the feathers of *Coracias Indica*, a bird common in Southern India, showed striking variation in color depending on the angle of incident light.[1] He hypothesized that this iridescence was due to ordering in structure barbs, though this idea was rejected when scanning electron microscopy in the 1940s seemed to reveal only random structures.

Raman's hypothesis ended up being revived thirty years later when Dyck managed to experimentally falsify aspects of the random distribution model.[1] He hypothesized that the color was constructive interference from an ordered matrix of vacuoles, but it was unknown if a weakly ordered, or "quasi-ordered" structure would be ordered enough to produce wavelength-specific-color.

Prum et. al. have provided evidence for order in the structures using Fourier analysis of electron micrographs of medullary keratin.[1] From their structural analysis they have been able to successfully predict the wavelengths of the optical reflection peak, showing that the colors do originate from the order in the structure.

1.2 Experimental Data

Prum et. al. have studied color production in the barbs for six avian species, including *Cotinga Cotinga* (*C. Cotinga*), which has barbs which consist of spher-

*emilie.huffman@my.uu.edu

ical air-cavities in a β-keratin background. For the barbs, they measured the scattering intensity as a function of wavelength, sample orientation, incident light angle, and viewing angle. They found that for natural daylight, the structure of *C. Cotinga* produced high intensity, regardless of incident angle, in the 400-500nm range. Using directional light produced some iridescence, but natural daylight caused non-iridescent scattering. This paper will model the arrays of spherical cavities found in *C. Cotinga* as arrays of dielectric non-overlapping spheres and calculate their scattering intensities as a function of incident angle, viewed angle, and wavelength.

2 Theory

2.1 T-Matrix Approach

The electromagnetic field formed from light incident on a grouping of dielectric objects can be written using longitudinal, magnetic, and electric potentials ψ_R^L, ψ_R^M, and ψ_R^E as:

$$E = \nabla\psi_R^L + \mathbf{L}_R\psi_R^M - \frac{i}{k}\nabla\times\mathbf{L}_R\psi_R^E \tag{1}$$

where $k=\omega/c$ and $\mathbf{L}=-i(r-\mathbf{R})\times\nabla$ is the orbital angular momentum operator relative to $\mathbf{R}$, the position vector.[5]

For a system with no nearby external source, $\psi_R^L=0$. The function ψ_R^E can be obtained using the following identity[3]:

$$\psi_\alpha^E = \frac{i}{k\epsilon_j\mu_j}\frac{1}{L_\alpha^2}\left(\mathbf{L}_\alpha\times\nabla\right)\cdot\mathbf{E} \tag{2}$$

For a grouping of dielectrics, the total electric field $\mathbf{E}$ is equal to $\mathbf{E}^{ext}+\mathbf{E}^{ind}$, where $\mathbf{E}^{ext}$ is the external field and $\mathbf{E}^{int}$ is the field induced by the scattering on the objects. Solving for the induced fields at each position $\mathbf{R}$ yields the following net scattering amplitude relation:

$$\begin{aligned}\mathbf{f}(\Omega) &= \sum_\alpha e^{-i\mathbf{k}'\cdot\mathbf{r}_\alpha}\sum_L\Big[\mathbf{X}_L(\Omega)\,\Psi_{\alpha,L}^{M,ind}/k_0 \qquad (3)\\ &\quad + \hat{\mathbf{r}}\times\mathbf{X}_L(\Omega)\,\Psi_{\alpha,L}^{E,ind}/k\Big] \qquad (4)\\ &\approx \sum_\alpha e^{-i\mathbf{k}'\cdot\mathbf{r}_\alpha}\sum_L\hat{\mathbf{r}}\times\mathbf{X}_L(\Omega)\,\Psi_{\alpha,L}^{E,ind}/k\end{aligned}$$

where $k=\omega/c$ and $\mathbf{X}_L=\mathbf{L}Y_L(\Omega)$ is the vector spherical harmonic. The sum over L requires a sum over the l-states, and thus the m-states for each l. The approximation in which the magnetic functions are neglected is made in the electric dipole scattering limit.

The plane wave describing the external field is given by $E^{ext}=\vec{\epsilon}e^{i\mathbf{k}\cdot\mathbf{r}}$, where $\vec{\epsilon}$ is the polarization of the light (assumed to be normalized.)[4] If this expression is expanded in spherical plane waves and combined with Equation 2, the coefficients of the electric scalar functions are found to be:

$$\psi_{\alpha,L}^{E,ext} = \frac{4\pi e^{i\mathbf{k}\cdot\mathbf{r}_\alpha}}{l(l+1)}\left[\mathbf{X}^*(\Omega_i)\cdot\frac{\vec{\epsilon}\times\mathbf{k}}{k\epsilon_0\mu_0}\right] \tag{5}$$

When (1) is inserted into Maxwell's equations, it is found that the scalar functions must satisfy the following wave equation[3]:

$$\left(\nabla^2+k_j^2\right)\psi=0 \tag{6}$$

where $k_j=k\sqrt{\epsilon_j\mu_j}$. This implies that the multipole expansion of the electromagnetic field in this region can be expressed as a sum of free spherical waves.[3] The external field can be written in terms of spherical harmonics and spherical Bessel functions.

For the system of dielectrics, the electromagnetic field in the medium can be represented as a combination of spherical Hankel functions: h_l^+ for outgoing waves and h_l^- for incoming waves. Because the sources of $\mathbf{E}^{ind}$ are induced by the external field in the dielectric objects, $\mathbf{E}^{ind}$ is expressed solely in terms of h_l^+, the outgoing functions.

In the linear response approximation for single scattering, the components of the scattered field (Ψ^{ss}) are proportional to those of the external field (Ψ^{ext}), so the following relationship holds:

$$\Psi^{ind}\approx\Psi^{ss}=t\Psi^{ext} \tag{7}$$

where the factor t is known as the scattering t-matrix. By solving Maxwell's equations in the presence of a dielectric object, using an asymptotic condition that forces ψ_L to equal the sum of the external and induced fields in terms of the t scattering matrix, the elements of such a matrix can be found for each L. De Abajo et. al. used such a method to determine the t-matrix for spherically symmetric objects, yielding[3]:

$$t_l^E = \frac{-j_l(\rho_0)\left[\rho_1 j_l(\rho_1)\right]'+\epsilon\left[\rho_0 j_l(\rho_0)\right]' j_l(\rho_1)}{h_l^+(\rho_0)\left[\rho_1 j_l(\rho_1)\right]'-\epsilon\left[\rho_0 h_l^+(\rho_0)\right]' j_l(\rho_1)} \tag{8}$$

where $\rho_0=ka$ and $\rho_1=ka\sqrt{\epsilon}$, and a is the radius of the spheres. The scattering amplitude from a coherent light source incident on a group of N dielectrics

can now be expressed as $\sum_{\alpha=1}^{N} \mathbf{f}_\alpha$, where $\mathbf{f}_\alpha$ is given by:

(9)

$$\mathbf{f}_\alpha(\theta,\phi,\theta_i,\phi_i) = 4\pi e^{i(\mathbf{k}-\mathbf{k}')\cdot\mathbf{r}_\alpha}$$
$$\sum_{l=1}^{\infty}\sum_{m=-l}^{l}\left(\frac{\hat{\mathbf{r}}\times\mathbf{X}_{l,m}(\theta,\phi)}{l(l+1)}\right)\left[t_{\alpha,l}\mathbf{X}^*_{l,m}(\theta_i,\phi_i)\cdot\frac{\vec{\epsilon}\times\mathbf{k}}{k^2\epsilon_0\mu_0}\right]$$

where $\mathbf{X}_{l,m}$ is given in spherical polar coordinates (Y_l^m is a spherical harmonic) by[7]:

$$\mathbf{X}_{l,m} \equiv \hat{\theta}\left\{\frac{-mY_l^m}{[l(l+1)]^{\frac{1}{2}}\,sin\theta}\right\} + \hat{\phi}\left\{\frac{-i}{[l(l+1)]^{\frac{1}{2}}}\frac{\partial Y_l^m}{\partial\theta}\right\} \quad (10)$$

The total scattering intensity is then obtained from $\mathbf{f}\cdot\mathbf{f}^*$, where $\mathbf{f} = \sum_{\alpha=1}^{N}$, and $\mathbf{f}_\alpha$ is given by (9). Note however that this result assumes the incident light is coherent.

2.2 Nearest Neighbor Approach

An alternative way of arranging the terms in an equation for the scalar scattering intensity ($\mathbf{f}\cdot\mathbf{f}^*$) is given by the equation below:

$$\mathbf{f}\cdot\mathbf{f}^* = \sum_{\alpha=1}^{N}|\mathbf{f}_\alpha|^2 + \sum_{\alpha\neq\beta}^{N^2-N}\mathbf{f}_\alpha\cdot\mathbf{f}^*_\beta \quad (11)$$

where $\mathbf{f}_i$ is given by (9).

In a randomly distributed assortment of scatterers it can be shown that the terms where $\alpha \neq \beta$ give a negligible contribution to the sum. [4] However, for a large collection of scatterers in some sort of regular distribution the contributions of the terms mixing $\mathbf{f}_\alpha$ and $\mathbf{f}_\beta$, where $\mathbf{r}_\alpha$ and $\mathbf{r}_\beta$ are sufficiently close, become important. Thus the equation becomes:

$$\mathbf{f}\cdot\mathbf{f}^* = \sum_{\alpha=1}^{N}|\mathbf{f}_\alpha|^2 + \sum_{\alpha\beta=\mathrm{nn}}\mathbf{f}_\alpha\cdot\mathbf{f}^*_\beta \quad (12)$$

where "nn" means the near neighbors for which light is coherent. The coherence length depends on the source, and for sunlight is about 600 nm[8]. The first sum in this equation will yield the same intensities as those for a single sphere multiplied by N, and will be referred to as the incoherent term, whereas the second sum will be referred to as the coherent term, as it contains the structural information of the particular system and creates its distinctive scattering pattern.

2.3 Multiple Scattering

The singly scattered field generated by a dielectric can, in general, be scattered additional times by all other dielectrics in the system. The equation for the induced field thus becomes

$$\Psi_\alpha^{ind} = \Psi_\alpha^{ss} + t_\alpha\sum_{\alpha\neq\beta}G_{\alpha\beta}\Psi_\beta'^{ind} \quad (13)$$

where G is Green's function.

The following recursion relation can be used to solve for the system in question

$$\Psi^n = \Psi^0 + t\sum G\Psi^{n-1}, (n>0) \quad (14)$$

and Green's function can be approximated using the Rehr-Albers separable approximation.[6]

3 Method

3.1 Structure

To approximate the structure factor for found in the paper by Prum et. al.[1], Vila generated Cartesian coordinates for 10,000 spheres distributed in an approximately 5418nm x 5418nm x 5418nm cube based on the hard sphere model. The figure below compares the structure factor for the generated structure to the one found experimentally by Prum et. al. for *C. Cotinga*.

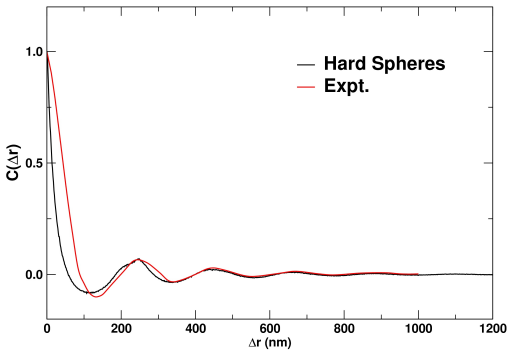

Figure 1: *The black line is the factor for the spheres generated by Vila, and the red is for the experiment.[1]*

3.2 Scattering Calculation

A program was written in C to read in the coordinates for the 10,000 spheres, and then calculate the scattering intensities for both the complete single-scattering

sum of all 10,000 spheres, and for the nearest neigbor approach. The spheres were given a radius of 120 nm, which is the spherical radius for *C. Cotinga*, and the dielectric constant assigned to the structure was 1.5. A plot of the t-matrix was made in *Mathematica* for increasing values of ℓ (Figure 2), and it was found that after the fourth term, the t-matrix dies off sufficiently to make any higher ℓ contributions on the scattering sum too minicule to consider. Thus the program went up to ℓ=4 for the calculations. For the nearest neighbor approach, only dielectrics located within three dielectric diameter lengths of each other were used in the calculation.

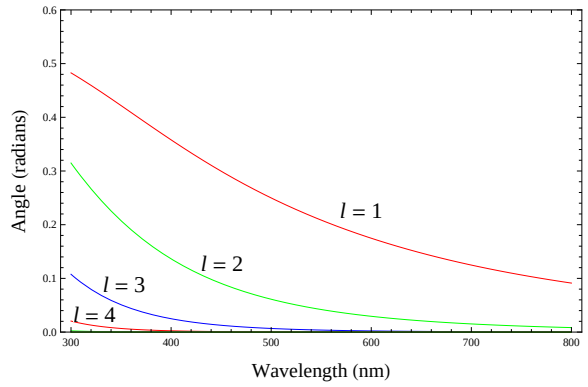

Figure 2: *The t-matrix as a function of wavelength for values of ℓ ranging from 1-4. As ℓ increases, the t-matrix curves die off.*

4 Results

4.1 Intensities from Entire Scattering Function

Figures 3 and 4 show the scattering in terms of scattered angle and wavelength of scattered directional light for one of the structures generated by Vila. Figure 3 is for light incident at an angle of $\pi/4$. It has strong intensity for light in the range of 400-500 nm, results consistent with those of Noh et. al.[1] However, there also appear to be a lot "speckles" or noise surrounding the major peak area. These are in different areas for each different incident angle and suggest some iridescence.

Figure 4 gives the scattering intensities for light incident at an angle of $\pi/2$. It also has a strong intensity for light in the range of 400-500 nm, and it can be seen that the "speckles" are still there, but positioned differently.

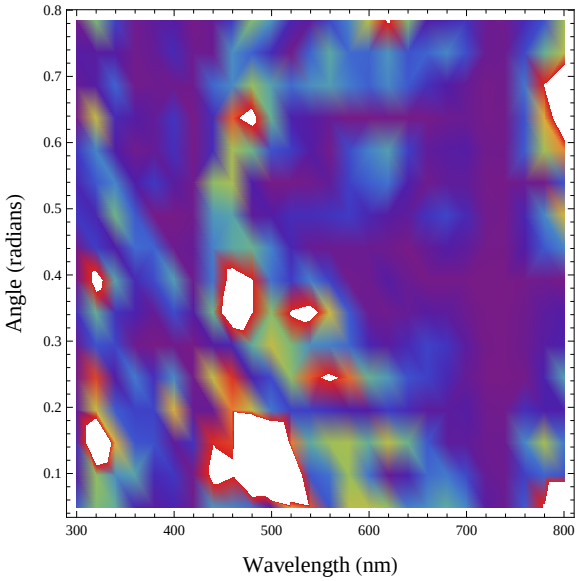

Figure 3: *The wavelength ranges from 300-800nm on the horizontal axis, and the theta from 0 to $\pi/4$ on the vertical axis. Calculations were made in increments of 20 nm and $\pi/64$ radians.*

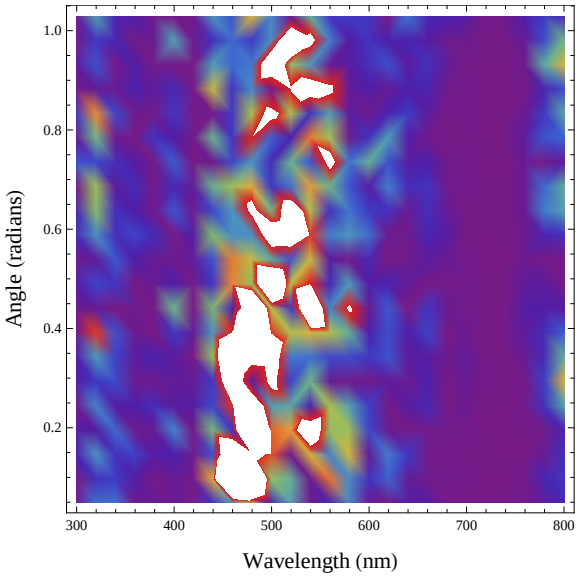

Figure 4: *The wavelength ranges from 300-800nm on the horizontal axis, and the theta from 0 to $\pi/4$ on the vertical axis. Calculations were made in increments of 20 nm and $\pi/64$ radians.*

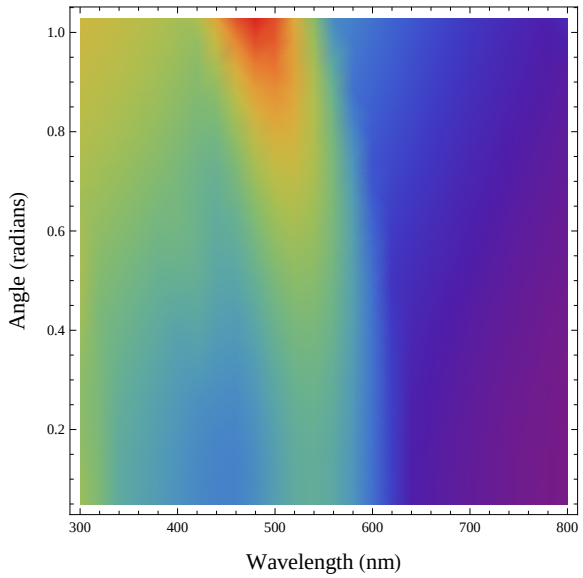

Figure 5: *The wavelength ranges from 300-800nm on the horizontal axis, and the theta from 0 to $\pi/4$ on the vertical axis. Calculations were made in increments of 20 nm and $\pi/64$ radians.*

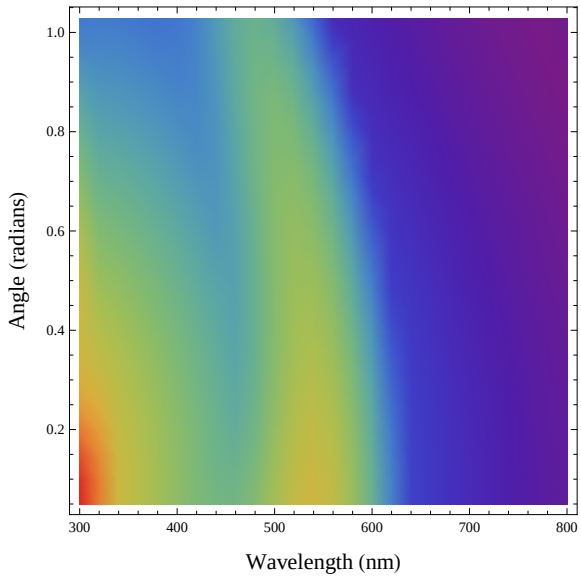

Figure 6: *The wavelength ranges from 300-800nm on the horizontal axis, and the theta from 0 to $\pi/4$ on the vertical axis. Calculations were made in increments of 20 nm and $\pi/64$ radians.*

Though experimentally the barbs show iridescence from directional lighting, the iridescence suggested by the noise in these images is too strong. It is doubtful that the interactions between the farthest structures in the cell actually contribute since they exceed the coherence length for visible light, but they are being used in this calculation.

4.2 Intensities from Near Neighbor Approach

Figures 5 and 6 give scattering results using the approach of (12) with three nearest neighbors. The coherent term was calulated only from dielectrics which were three diameter lengths away from each other. In both figures it is evident that the intensity the intensity peaks for the wavelength range of 400-600 nm, but there are no "speckles," and there is more continuity in the images.

Figure 5 gives the backscattered intensities assuming an incident light angle of $\pi/2$ in the theta direction, as well as incident and scattered angle $\phi = 0$. The vertical axis gives the angle between the incident and backscattered light, which is being varied in the theta direction. The highest intensity is in the higher angle and 400-500 nm range, a finding inconsistent with experiment, which show a peak in the low angle range.

Figure 6 gives the backscattered intensities assuming an incident light angle of $\pi/2$ in the theta direction, as well as incident $\phi = 0$. The vertical axis gives the angle between the incident and backscattered light, which is being varied in the phi direction. The highest intensity is in the 500-600 nm range, a finding inconsistent with experiment, which show a peak in the 500-600 nm range.

5 Conclusions

Both attempts to calculate intensity resulted in plots with the strongest intensity in the 400-600 nm range, results consistent with the experimental data of Noh, et. al. The calculation involving the interactions of all the dielectrics in the region had some noise, suggesting iridescence. The calculation involving only interactions between dielectrics a few wavelengths apart yielded intensity only in the 400-600 nm region, without the additional noise. This is consistent with experiment, however, the phi-dependence is inconsistent and stems from assuming a polarization in light. This should be corrected by averaging over all polarizations. All calculations revealed high intensity scattering in distinct visible wavelength ranges, giving a theoretical basis for visible wavelength specific scattering in quasi-ordered structures.

6 Future Work

There are many additional considerations that can be taken into account for future work on this project. The phi-dependence must me removed by averaging over all polarizations. The code generated for the results in this paper only uses the single-scattering formula, and multiple-scattering may be important for modeling this system accurately. Also, the proteins being modeled are not dielectric spheres, but rather spherical cavities in a dielectric material, this would suggest a need to modify the t-matrix.

7 Acknowledgements

I would like to thank Fernando D. Vila and John J. Rehr for their guidance in this project–for directing me to helpful papers and other materials, and for debugging aid/advice. In addition, Vila generated the structures to match those of *C. Cotinga*. Takimoto and Low developed much of the theory used in this project. This project was funded by the National Science Foundation: award number 1062795. Finally, I would like to thank fellow REU students Arman, Charlie, Gina, Megan, and Micah for their support this summer.

References

[1] Noh, Heeso; Liew, Seng Fatt; Saranathan, Vinodkumar; Mochrie, Simon G. J.; Prum, Richard O.; Dufresne, Eric R.; and Cao, Hui. *How Noniridescent Colors Are Generated by Quasi-ordered Structures of Bird Feathers*. Advanced Materials, *1*, XX, (2010).

[2] Noh, Heeso; Liew, Seng Fatt; Saranathan, Vinodkumar; Mochrie, Simon G. J.; Prum, Richard O.; Dufresne, Eric R.; and Cao, Hui. *Double scattering of light from Biophotonic Nanostructures with short-range order*. (2010). Optics Express. Vol. 18, No. 11, 11948.

[3] De Abajo, F. J. Garcia, *Multiple Scattering of Radiation in Clusters of Dielectrics*. Physical Review B. Vol. 60, No. 8 (1999).

[4] Jackson, John David. Classical Electrodynamics, Third Edition. John Wiley and Sons, Inc. 1999.

[5] Takimoto, Yoshi and Rehr, John J. *Multiple Scattering of Light from Dielectric Spheres*. University of Washington. (2004).

[6] Rehr, John J. and Albers, R. C. *Theoretical Approaches to X-Ray Absorption Fine Structure*. Review of Modern Physics. Vol. 73, No. 3, (2000).

[7] Hill, E. L., *The Theory of Vector Spherical Harmonics*, University of Minnesota, 1953.

[8] Engineering Physics, Vol. 19, 245 (98).